



# Immunoreactivity profiling of Anti-Chinese hamster ovarian host cell protein antibodies by isobaric labeled affinity purification-mass spectrometry reveals low-recovery proteins

Shunsuke Takagi<sup>a,b</sup>, Masayoshi Shibata<sup>b</sup>, Nobuyuki Suzuki<sup>b</sup>, Yasushi Ishihama<sup>a,c,\*</sup>

<sup>a</sup> Department of Molecular Systems BioAnalysis, Graduate School of Pharmaceutical Sciences, Kyoto University, Kyoto 606-8501, Japan

<sup>b</sup> Analytical and Quality Evaluation Research Laboratories, Daiichi Sankyo Co., Ltd., Hiratsuka, Kanagawa 254-0014, Japan

<sup>c</sup> Laboratory of Clinical and Analytical Chemistry, National Institute of Biomedical Innovation, Health and Nutrition, Ibaraki, Osaka 567-0085, Japan

## ARTICLE INFO

### Article history:

Received 5 September 2022

Revised 8 November 2022

Accepted 9 November 2022

Available online 11 November 2022

### Keywords:

Host cell proteins (HCPs)

Liquid chromatography/mass spectrometry (LC/MS)

Affinity purification

Isobaric labeling

Biopharmaceutics

## ABSTRACT

We evaluated the immunoreactivity profiles of eight commercial anti-host cell protein (anti-HCP) antibodies from different host animals and their antigens used for immunization by an isobaric labeled affinity purification-mass spectrometry (AP-MS) method. As a result, 34 proteins with high abundance but low recovery from harvest cell culture fluid were identified. Since they are likely to be underestimated in biopharmaceutical quality assessment, the features common to these proteins were investigated. Compared to other immunoprecipitated HCP proteins, proteins exhibiting lower molecular weight ( $\Delta MW = -14600$ ), lower isoelectric point ( $\Delta pI = -0.86$ ), and lower hydrophobicity ( $\Delta GRAVY = -0.13$ ) were enriched. This AP-MS method provides important information for HCP control strategies using immunological methods and is expected to contribute to the development of safe biopharmaceutics.

© 2022 The Authors. Published by Elsevier B.V.

This is an open access article under the CC BY license (<http://creativecommons.org/licenses/by/4.0/>)

## 1. Introduction

Host cell proteins (HCPs) are proteins derived from host cells used in the production of biopharmaceuticals, and may be present as impurities in the final products [1–3]. Because of their toxicity and immunogenicity to humans [4–6], and/or their potential for degradation of products and additives due to their enzymatic activities [7–11], they are required by regulatory authorities to be controlled at low levels. Since HCPs are complex mixtures of proteins, sandwich enzyme-linked immunosorbent assay (ELISA) methods using a mixture of antibodies reactive to various HCPs are widely employed for HCP analysis [12–14]. ELISA methods using anti-HCP antibodies are highly specific and sensitive, allowing high-throughput analysis of a wide range of HCPs [15], and providing a single result of relative reactivity with respect to a mixture of HCPs used as standards [14]. Even though modern high-performance liquid chromatography/mass spectrometry (LC/MS) approaches have been reported to be applicable to HCP analysis [16–20], ELISA methods are still exclusively used in quality control testing because of this ease of handling [21].

*Abbreviations:* HCCF, Harvest cell culture fluid; HCP, Host cell protein; AP-MS, Affinity purification-mass spectrometry; iLAP-MS, Isobaric labeling AP-MS.

\* Corresponding author.

E-mail address: [yishiham@pharm.kyoto-u.ac.jp](mailto:yishiham@pharm.kyoto-u.ac.jp) (Y. Ishihama).

Anti-HCP antibodies used in ELISA methods are required to react with a wide range of HCPs to minimize the risk of overlooking residual HCPs in the products [14,21]. The degree of comprehensiveness of the anti-HCP antibody against the proteome to be analyzed is generally referred to as “coverage”, which is one of the most important parameters for ELISA methods [1,21]. Traditionally, two-dimensional gel electrophoresis (2-DE) has been used for coverage assessment. However, overlapped protein spots due to the incompleteness of separation by 2-DE can lead to misinterpretation of the immunoreactivity [21–25]. As alternatives, several LC/MS methods have been utilized to comprehensively profile the immunoreactivity of anti-HCP antibodies by analyzing proteins purified by anti-HCP antibodies [26–30].

An essential step in this affinity purification-MS (AP-MS) method is to distinguish immunoreactive proteins from nonspecific binding proteins. Henry et al. first reported a method that relied solely on identification information to judge all proteins identified from negative controls as nonspecific binders, but in the same report, they noted that identification-based methods have a high risk of false-negative results and they commented on the need for quantitative information [26]. Many of the AP-MS studies reported since then have used quantitative information to determine immunoreactivity, but all of them have employed label-free quantification (LFQ), which is difficult to perform accurately due to matrix effects [27,28]. Thus, despite their importance, little attention has

been paid to the precision and accuracy of quantitative methods. The AP-MS method is expected to extract data that cannot be obtained with the conventional 2-DE method by performing relative quantitation not only between affinity-purified samples and negative controls, but also between affinity-purified samples prepared using different anti-HCP antibodies and between pre- and post-affinity-purified samples. Therefore, the development of an AP-MS method with better quantitative performance would be advantageous.

Stable isotope labeling methods based on metabolic and chemical reactions provide high quantitative performance in proteomics [31–34]. Among them, isobaric labeling is expected to greatly improve the quality of results obtained from AP-MS, since it allows relative quantitation of many samples within the same measurement [35–37]. In this study, we combined an AP-MS workflow using anti-Chinese hamster ovarian (CHO) cell HCP antibodies and magnetic beads with a quantitative proteomics method using tandem mass tag (TMT) labeling to establish a workflow that overcomes the challenges of the classic LFQ-based AP-MS methods that have been utilized to date. TMT labeling is suitable for simultaneous analysis of multiple samples and negative controls because of its high-throughput performance, with a maximum of 11-plex for conventional TMT reagents and 18-plex for the recently developed TMTpro reagents [32,38]. We first evaluated the impact of the introduction of isobaric labels on the AP-MS method in terms of quantitative precision. Furthermore, the developed workflow was applied to a comparative analysis of eight commercially available anti-HCP antibodies produced by different host animals immunized with various antigens, and succeeded in identifying low-recovery “alert proteins” for HCP-ELISA.

## 2. Materials and methods

### 2.1. Materials

Triethylammonium bicarbonate buffer pH 8.5 (TEAB), rabbit IgG, and goat IgG were purchased from Merck KGaA (Darmstadt, Germany). Modified trypsin was obtained from Promega Corporation (Madison, WI). Phosphate-buffered saline (PBS) and phosphate-buffered saline with Tween 20 (PBST) were purchased from Takara Bio Inc. (Shiga, Japan). Dynabeads protein G, bis(sulfosuccinimidyl)suberate (BS<sup>3</sup>), and TMT reagents were purchased from Thermo Scientific (Waltham, MA). Protein G sensor chip, HBS-EP+ (10 mmol/L 4-(2-hydroxyethyl)-1-piperazineethanesulfonic acid (HEPES), 150 mmol/L NaCl, 3 mmol/L ethylenediaminetetraacetic acid (EDTA), and 0.05 v/v% surfactant P20, after diluted), and glycine buffer pH 1.5 were purchased from Cytiva (Tokyo, Japan). Recombinant phospholipase B-like 2 protein (PLBL2) and cathepsin D of Chinese hamster were purchased from ICL (Portland, OR) and MyBioSource (San Diego, CA), respectively. Information on antibodies used for affinity purification is shown in Suppl. Table 1. Other reagents were obtained from Fujifilm Wako (Osaka, Japan). Mock CHO-O cells, produced by transfection with a vector that does not contain genes of interest, were cultured and the collected harvest cell culture fluid (HCCF) was used as a sample. The CHO-O cell line was established as previously reported [39].

### 2.2. Affinity purification

Protein G magnetic beads (Dynabeads protein G) were used for affinity purification. Three types of immobilized beads for affinity purification were prepared as follows; 1) beads with immobilized anti-HCP antibody (anti-HCP antibody beads), 2) beads with immobilized goat or rabbit nonspecific antibody (antibody blank beads),

and 3) non-treated beads (naked blank beads). Antibody immobilization on beads was performed by suspending 60  $\mu$ g of antibody and 7.5 mg of beads in 400  $\mu$ L of PBST and allowing the beads to react for 60 min at room temperature. After the reaction, the solution was discarded and the immobilized beads were washed with PBST to remove unbound antibody. Naked blank beads were prepared similarly by adding the beads to PBST. Immobilized beads were prepared for each affinity purification experiment.

Covalent conjugation of antibodies to beads were performed by adding 700  $\mu$ L of PBS containing crosslinking reagent (BS<sup>3</sup>) to the immobilized beads, followed by 30 min incubation at room temperature. After the incubation, 25  $\mu$ L of 1 mol/L Tris-HCl buffer (pH 7.5) was added and incubated for 15 min at room temperature to stop the reaction. Treated beads were then washed with PBST. The crosslinking reaction was performed temporarily during the method development process.

Affinity purification was performed by adding 400  $\mu$ L of PBST containing 100  $\mu$ g of protein from HCCF to the immobilized beads, followed by incubation overnight at 5°C. After the reaction, the solution was discarded and the beads were washed with PBS. To elute the protein from the beads, 100  $\mu$ L of phase transfer surfactant (PTS) solution (12 mmol/L sodium deoxycholate, 12 mmol/L sodium N-dodecanoylsarcosinate, 0.2 mol/L TEAB), which is compatible with trypsin digestion, was added and the beads were heated at 95°C for 5 min [40].

For anti-HCP antibody beads, affinity purification was repeated three times for each antibody. For blank beads (antibody blank beads and naked blank beads), the affinity purification was repeated four times and the eluate was combined in a single tube. This solution was again divided into four aliquots and subjected to the following protein digestion procedure.

### 2.3. Protein digestion

Eluates from the beads were reduced (10 mmol/L dithiothreitol, 37°C, 30 min) and alkylated (50 mmol/L iodoacetamide, 37°C, 30 min in the dark) prior to enzymatic digestion. The treated proteins were incubated with Lys-C for 3 hours, diluted 5-fold with 50 mmol/L ammonium bicarbonate, and further digested with trypsin overnight. After digestion, the solution was acidified with trifluoroacetic acid (TFA) and the surfactant was removed from the solution by extraction with ethyl acetate. The recovered aqueous layer containing the peptide was desalted on a StageTip packed with SDB-XC (CDS Analytical LLC, Oxford, PA) to obtain 50  $\mu$ L of eluate [41].

### 2.4. Preparation of whole HCCF digest

HCCF corresponding to 100  $\mu$ g of protein was added to 100  $\mu$ L of PTS solution and heated at 95°C for 5 min. Subsequent reduction-alkylation, digestion, surfactant removal, and desalting operations were performed as described above for the affinity-purified samples to prepare the “whole HCCF digest”.

### 2.5. TMT labeling and sample solution preparation

All peptides recovered by affinity purification and 10  $\mu$ g of the whole HCCF digest were subjected to TMT labeling. TMT labeling was performed according to the manufacturer’s standard protocol. The peptides were completely dried and reconstituted in 100  $\mu$ L of 50 mmol/L TEAB. TMT 11-plex labeling reagents (0.8 mg) were dissolved in 41  $\mu$ L of acetonitrile and the entire volume was added to the peptide solutions. The solutions were allowed to react for 1 hour at room temperature. The reaction was quenched by adding 8  $\mu$ L of 5% hydroxylamine solution and incubating for 15 min. After quenching, the acetonitrile concentration of the solutions was

diluted to 4% by adding 0.1% TFA and the mixtures were desalted as described previously to yield 50  $\mu\text{L}$  of eluates. TMT batches were prepared by combining 20  $\mu\text{L}$  of each TMT-labeled peptide as shown in Suppl. Table 2. The mixtures were concentrated to dryness and the residues were dissolved in 133  $\mu\text{L}$  of sample loading buffer (4% acetonitrile, 0.1% TFA) to prepare a sample solution for LC/MS analysis.

To prepare the unlabeled affinity-purified samples for evaluating LFQ, 20  $\mu\text{L}$  of the desalted digest was concentrated to dryness and dissolved in 133  $\mu\text{L}$  of sample loading buffer.

## 2.6. LC/MS analysis

LC/MS analyses were performed using an UltiMate 3000 RSLC-nano pump (Thermo Fisher Scientific) coupled to an Orbitrap Fusion Lumos mass spectrometer (Thermo Fisher Scientific). The sample solution (5  $\mu\text{L}$ ) was injected directly into the analytical column. Separation was performed using an EASY-Spray column (Thermo Fisher Scientific) with an inner diameter of 75  $\mu\text{m}$  and a length of 500 mm, packed with C18 modified silica gel (2  $\mu\text{m}$  particle size). The column temperature was maintained at 50°C during the analysis. The following solutions were used as mobile phases: solution A: 0.5% acetic acid, solution B: 80% acetonitrile, 0.5% acetic acid. The gradient was 5% B to 40% B for 240 min, with a constant flow rate of 300 nL/min. The voltage applied to the spray emitter was 2.2 kV.

TMT-labeled samples were analyzed by data-dependent acquisition (DDA) in top speed mode with a cycle time of 5 s. Survey scans were acquired by the Orbitrap with the following parameters: an  $m/z$  range of 375 to 1500, a resolution of 120,000, and an automatic gain control (AGC) of  $4.0 \times 10^5$ . MS<sup>2</sup> acquisition was performed by collision-induced dissociation (CID) using an ion trap, and the collision energy for CID was set to 35%. Ions were isolated with quadrupoles in a 0.7  $m/z$  window; AGC was set to  $1.0 \times 10^4$ , maximum injection time was 35 ms, and scan rate was set to "Turbo." The MS<sup>3</sup> analysis was performed after co-isolation of the top 10 product ions observed in the MS<sup>2</sup> analysis by synchronous precursor selection using an ion trap. Isolated ions were fragmented by higher-energy collisional dissociation (HCD) with a HCD collision energy set at 65%, and TMT reporter ions were detected by the Orbitrap. The AGC was set to  $5.0 \times 10^4$  and the maximum injection time was 86 ms. All sample solutions were measured in triplicate.

Data for unlabeled samples were acquired by DDA in top speed mode with a period of 3 s. Survey and MS<sup>2</sup> scans were acquired with the Orbitrap and an ion trap, respectively. Survey scans were acquired with the same parameters as for TMT-labeled samples. Fragmentation was performed by HCD with an HCD collision energy of 27%. Parameters were set as follows; isolation window to 1.2  $m/z$  (quadrupole), AGC to  $1.0 \times 10^4$ , maximum injection time to 35 ms, and scan rate to "Rapid".

Experimental settings different from those described above during the method development process are described individually in the following section.

## 2.7. Raw data processing

Data acquired by the mass spectrometer were analyzed using Proteome Discoverer ver. 2.2.0.388 (Thermo Fisher Scientific). For the immunoreactivity evaluation and cluster analysis, raw files of triplicate runs were combined into one raw file using the fraction management function of Proteome Discoverer to reduce missing values. For the evaluation of the variability of LC/MS measurements, raw files were analyzed individually to obtain quantitative values for each run separately.

**Table 1**

Number of immunoreactive proteins identified at different thresholds using the iLAP-MS method

Anti-HCP antibody	No. of immunoreactive proteins			No. of quantified proteins
	Judged by q-value <sup>a</sup>		Judged by enrichment ratio (2-fold)	
	$\leq 0.05$	$\leq 0.01$		
BioGenes Type A	931	664	560	1092
BioGenes Type B	1002	775	796	1080
BioGenes Type C	1061	998	811	1100
BioGenes Type D	1052	959	857	1090
Cygnus 1G	777	546	316	1041
Cygnus 3G	1035	962	842	1077
Cytiva	870	463	458	1043
Canopy	859	665	355	996

<sup>a</sup> q-value was calculated from three independent affinity purification procedures as described in the materials and methods section

Data was searched against the UniProtKB release 2021\_01 (7th April, 2021) Chinese hamster database (56495 sequences) and the common contaminants database by the Sequest HT engine. Search parameters were set as: precursor mass tolerance of 5 ppm, product ion mass tolerance of 0.6 Th, trypsin enzyme, minimum peptide length of 6, allowing up to 2 missed cleavages. For TMT-labeled samples, carbamidomethylation of Cys, TMT labeling of peptide N-terminus and Lys were set as static modifications. Oxidation of Met and acetylation of protein N-terminus were set as variable modifications. The false discovery rate (FDR) of the peptide spectral match (PSM) was determined by a target-decoy strategy using a reversed-sequence decoy database and controlled by Percolator software. The threshold for the FDR to filter PSM was set at a q-value of 0.01. For protein identification, the threshold for protein FDR was set at 0.01, and at least two peptides, including at least one unique peptide, were required to be identified. For the unlabeled samples, the same settings as for the TMT-labeled samples were used, except for the TMT modification. Two immunoglobulins (A0A3L7GXT6 and A0A3L7H109) that were artifacts derived from the reagent antibodies were excluded from subsequent analyses.

Signal-to-noise (S/N) ratios of TMT reporter ions in MS<sup>3</sup> spectra were employed as quantitative values for TMT-labeled samples. LFQ using peak area of extracted ion chromatogram (EIC) was applied to unlabeled samples. Protein abundances were obtained by summing the quantitative values for unique and razor peptides belonging to the corresponding proteins both for TMT and LFQ.

## 2.8. Statistical assessment of immunoreactivity

Perseus ver. 1.6.14.0 was used for the statistical assessment of immunoreactivity [42]. Within each TMT batch, the enrichment rate (Sp/Blank) was determined using anti-HCP antibody as the numerator and the blank beads corresponding to the host animal of the anti-HCP antibody as the denominator. Then the enrichment rate was converted to  $\log_2$  (Sp/Blank). Mean  $\log_2$  (Sp/Blank) of each individually prepared sample ( $n = 1$  to 3) was calculated between the corresponding TMT batch pairs, since each anti-HCP antibody was measured in two TMT batches as summarized in Suppl. Table 2. Student's two-tailed t-test was performed on the data from three replicate preparations of affinity-purified samples to see if  $\log_2$ (Sp/Blank) was significantly different from 0. Significance levels were set by Benjamini-Hochberg's FDR, and q-value thresholds are shown in the text and in Table 1 [43]. If the q-value threshold was satisfied, the protein that met the criteria was judged to be immunoreactive with the corresponding anti-HCP antibody.

## 2.9. TMT data normalization

Raw protein abundance data were normalized prior to the cluster analysis to mitigate the TMT batch effect by using the previously reported technique (internal reference scaling (IRS) method) with some modifications [44]. First, to correct the amount of sample loaded per channel within a TMT batch, the sum of the protein abundance for each channel was normalized to that of the whole HCCF digest channel. Then, the geometric mean of the abundance of each protein was calculated for a total of 16 channels of whole HCCF digests (2 channels per batch, 8 TMT batches in total). From the aforementioned geometric mean and whole HCCF digests belonging to each individual TMT batch, correction factors for each protein per TMT batch were obtained. Finally, normalized abundance was obtained by normalizing the raw abundance of each protein using the correction factors for channels other than the whole HCCF digest in each individual TMT batch.

## 2.10. Cluster analysis

Perseus ver. 1.6.14.0 was used to perform hierarchical cluster analysis for  $\log_2$  (normalized abundance). Euclidean distances were used for both rows (proteins) and columns (samples), and the k-means method was used. The initial number of clusters was set to 300, the maximum number of iterations to 10, and the number of restarts to 1. Proteins with no missing quantitation values in all samples were included in the analysis (884 proteins).

## 2.11. Bioinformatics analysis

Hydrophobicity (GRAVY) and *in vivo* protein instability (instability index) were calculated by Biopython ver. 1.78 using an in-house Python script [45,46]. Molecular weight and *pI* were determined by Proteome Discoverer.

In this study, we introduced the “coverage-similarity score”, an index calculated from basic local alignment search tool (BLAST) search results, to evaluate the similarity of each corresponding protein between the CHO cell HCP and the host animal with a single value. BLAST searches were performed in a local environment using BLASTp included in the BLAST+ ver. 2.6.0 package [47,48]. UniProt Rabbit (downloaded June 2021, 41459 sequences in total) and UniProt Goat (downloaded June 2021, 35493 sequences in total) were used as the goat and rabbit databases, respectively. The protein sequences of CHO cells were used as queries, and the Top 1 hits were used as the homologs of the respective proteins for further analysis. Although the results were not filtered by E-value to avoid missing values, the percentages of hits with E-values greater than  $1 \times 10^{-3}$  were 0.3% and 1.2% for goat and rabbit, respectively, indicating that sufficiently significant hits were used for the analysis (denominator: 1151 proteins). The coverage-similarity score (CovSim score) was designed to reflect both length and similarity of the aligned sequences in a single value and was calculated using the following formula

$$\text{CovSim score} = \text{Query coverage (\%)} \times \text{Similarity (\%)} / 100$$

(1) where Query coverage (%) is defined as length of aligned subsequences in a BLAST search as a percentage of the length of the total query sequence, and Similarity (%) is defined as the extent to which aligned query and database protein sequences are related.

## 2.12. Statistical analysis

Hypothesis testing was performed using JMP ver. 16.0.0 (SAS Institute Inc., Cary, NC). The test methods and significance levels used are presented with the results. The family-wise error rate was controlled by the Holm-Bonferroni method [49].

## 2.13. Surface plasmon resonance analysis

Surface plasmon resonance (SPR) analyses were performed using a Biacore T200 system (Cytiva) and protein G sensor chip, with HBS-EP+ as a running buffer. Anti-HCP antibodies were captured on an active flow cell as ligands (20  $\mu\text{g/mL}$ , 300 s, 5  $\mu\text{L/min}$ ) and a flow cell without antibodies was used as a reference. For both of PLBL2 and cathepsin D, 2-fold dilutional series ranging from 0.625  $\mu\text{g/mL}$  to 10  $\mu\text{g/mL}$  (5 concentrations) were employed as analyte solutions. Association and dissociation time were 600 s and 300 s, respectively. Flow rate was 10  $\mu\text{L/min}$  and, sensor temperature was kept at 25°C during the analysis. Regeneration of the chip surface was conducted by injecting glycine buffer pH 1.5 for 30 s. Acquired data were evaluated by Biacore T200 evaluation software ver 3.0 (Cytiva).

## 3. Results and discussion

### 3.1. Performance and characteristics of the iLAP-MS method

In this study, we developed a novel isobaric labeling AP-MS (iLAP-MS) method employing TMT labeling to overcome the challenges of conventional LFQ-based AP-MS methods and we evaluated the performance and characteristics of the iLAP-MS method.

In affinity purification experiments, antibodies are often immobilized on magnetic beads with crosslinking reagents to selectively collect bound proteins while keeping the antibodies on the magnetic beads. The optimal concentration of crosslinking reagent (BS<sup>3</sup>) for immobilizing anti-HCP antibodies on magnetic beads was investigated by varying the concentration of crosslinker in the range of 0 to 5 mmol/L (5 mmol/L is the manufacturer's recommended condition). Surprisingly, the highest protein identification number and recoveries were obtained when the crosslinking reagent was not added (Suppl. Fig. 1). This may be due to inactivation of anti-HCP antibodies by the crosslinking reagent. Based on these results, we decided not to immobilize anti-HCP antibody on magnetic beads by crosslinkers. Next, we examined whether MS2 or MS3 spectrum was used for TMT quantification. Obtained results indicated that the distribution of  $\log_2$  (Sp/Blank) was lower for all four anti-HCP antibodies used in the evaluation when MS2 quantification was performed in comparison with MS3 quantification (Suppl. Fig. 2). This would be due to the large amount of anti-HCP antibody eluted from the magnetic beads, causing the isolation interference of precursor ions. Consequently, MS3-based TMT quantification using non-crosslinked antibodies were employed for accurate TMT quantification through this study.

One of the most critical issues with LFQ is that it directly reflects sample injection variability in LC/MS. However, by introducing isobaric labeling and performing the quantitation within the same LC/MS run, the precision can be improved. To evaluate the variability of LC/MS measurements for LFQ, an affinity-purified sample was injected in triplicate (LFQ\_inj), and to estimate the total variability of “preparation + measurement”, a single analysis was performed on each sample prepared in triplicate (LFQ\_prep). The median relative standard deviations (RSDs) of the peak area for LFQ\_inj and LFQ\_prep were 8.8% and 11.9%, respectively, indicating that the main source of variation in these results was the LC/MS analysis (Fig. 1). Similar to LFQ\_prep, we evaluated the total variability in TMT quantitation by analyzing samples prepared in triplicate, and the median RSD of the S/N value was determined to be 3.2% (TMT\_prep). The narrower distribution and smaller median RSD for TMT\_prep compared to LFQ\_inj, which does not include variation in sample preparation, indicates that the introduction of the isobaric label greatly improves the precision of the AP-MS method.

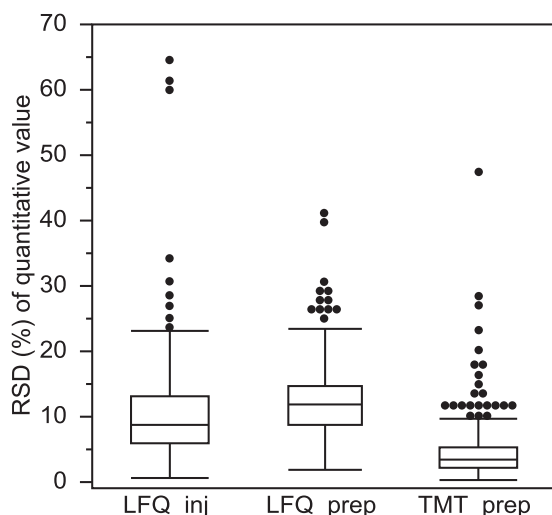


**Fig. 1.** Reproducibility in label-free and isobaric tag-labeled quantitation methods. The results for each series were obtained from the following measurements. LFQ\_inj: Triplicate LC/MS analyses of the same sample, LFQ\_prep: Single LC/MS analysis of each preparation in triplicate, TMT\_prep: Single LC/MS analysis of one TMT-labeled sample with three different channels for triplicate preparations (Batch 3-1 described in Suppl. Table 2). Proteins obtained by affinity purification using anti-HCP antibody (Cygnus 3G) were used as samples. For RSD calculation, peak area was used for label-free quantitation, whereas the reporter ion intensity (S/N value) was used for TMT quantitation. Commonly identified proteins were selected for the reproducibility comparison (356 proteins).

Next, TMT-labeled affinity-purified samples were prepared in triplicate and analyzed by LC/MS to obtain the TMT ratios, or enrichment rates (Sp/Blank), for eight commercially available anti-HCP antibodies. Then, q-values were calculated to identify proteins that were significantly enriched relative to the blank. As a result, more HCPs were identified when the q-value threshold was set at 0.05 than when the cutoff was set at the enrichment rate of 2.0-fold commonly used in previous studies (Table 1) [27,28]. Furthermore, even when the q-value threshold was tightened to 0.01, more immunoreactive proteins could be identified for all anti-HCP antibodies except for BioGenes Type B, which showed higher variability than the others (Table 1). These results indicate that the use of the high-precision iLAP-MS method in combination with the q-value threshold can increase the detection sensitivity in immunoreactivity profiling as compared with conventional determination methods while ensuring high reliability. The immunoreactivity of these anti-HCP antibodies was further evaluated by SPR method using two well-known problematic HCPs (PLBL2 and cathepsin D) [6,7]. The results showed that the selectivity of both methods was highly correlated (Suppl. Fig. 3), supporting the validity of the iLAP-MS method.

In general, the higher the protein recovery of an antibody, the more stable the quantitation and the higher the quantitation precision. However, when the correlation between protein recovery and quantitation precision by this iLAP-MS method was examined for the eight antibodies used in this study, the correlation coefficient was  $-0.239$ , which is surprisingly low (Suppl. Fig. 4). The AP-MS method for HCP has been widely used not only for the coverage assessment of anti-HCP antibodies, but also as an analytical technique to enrich and efficiently detect HCPs from biopharmaceuticals [50]. Thus, when selecting the appropriate anti-HCP antibody for each application, it is important to consider the possibility that an anti-HCP antibody with high protein recovery would not necessarily afford high precision.

### 3.2. Strategies for establishing appropriate negative controls

In affinity purification experiments, the selection of appropriate negative controls is important to minimize false positives. The "blank beads" used as a negative control could be beads with immobilized nonspecific antibodies that should ideally have no affinity for HCP, or "naked" beads on which nothing is immobilized. To determine the appropriate negative control, we focused our analysis on the "blank beads" data obtained by the iLAP-MS method. Suppl. Fig. 5 shows the protein recoveries for all affinity-purified samples, including the blank beads. In contrast to the amount of protein recovered from antibody blank beads with nonspecific antibodies from goat and rabbit, only a very small amount of protein was recovered from the naked blank beads. Interestingly, this result was contrary to that obtained in previous studies: according to Henry et al. [26], about 2.5 times more proteins were identified from "naked" beads than from beads immobilized with nonspecific antibodies. One possible reason for these results is the difference in the type of beads used for affinity purification. In the previous study, streptavidin-immobilized magnetic beads were used, whereas magnetic beads coated with protein G were used in this study. Therefore, when protein G beads are used, antibody blank beads are the appropriate negative controls and naked blank beads should not be employed in order to avoid overestimating the performance of anti-HCP antibodies. Our findings may indicate that protein G beads are more likely to suppress nonspecific adsorption of proteins on the beads, compared with the streptavidin beads.

When we evaluated the correlations of recovery for individual proteins between anti-HCP antibodies and nonspecific antibodies (goat and rabbit), all anti-HCP antibodies showed a higher correlation with nonspecific antibodies derived from the corresponding host animals (Suppl. Table 3). This result suggests that there are differences in the tendency for nonspecific adsorption to antibodies among host animal species. Therefore, the use of antibody blank beads matched to the host animal of the anti-HCP antibody as a negative control is considered to be important to accurately evaluate the coverage of anti-HCP antibodies.

### 3.3. Identification of problematic HCPs for ELISA analysis

In ELISA analysis for HCP, antigens with low affinity for the antibodies often cause problems such as inaccurate quantitation and low analytical precision. To identify such problematic proteins, we applied the iLAP-MS method to analyze the HCCF as well as affinity-purified samples prepared from eight commercially available anti-HCP antibodies. The results were subjected to cluster analysis after normalizing the protein abundances in the HCCF and affinity-purified samples (Fig. 2a). The amount of each protein recovered with each antibody correlated well with the amount in HCCF in most cases. However, there were 34 proteins that were recovered in small amounts by affinity purification despite the presence of large amounts in the HCCF (Fig. 2b, Suppl. Table 4). Proteins present in large amounts in the HCCF are more likely to remain as impurities after the biopharmaceutical purification process, and they must be accurately quantified [51]. Therefore, the "high abundance but low recovery" proteins extracted by cluster analysis are considered to be a group of proteins that are important but difficult to measure in HCP analysis using ELISA, and require careful consideration. The development of the iLAP-MS method, which enables accurate quantification, has enabled us to identify such "low-recovery HCPs" for the first time, to our knowledge.

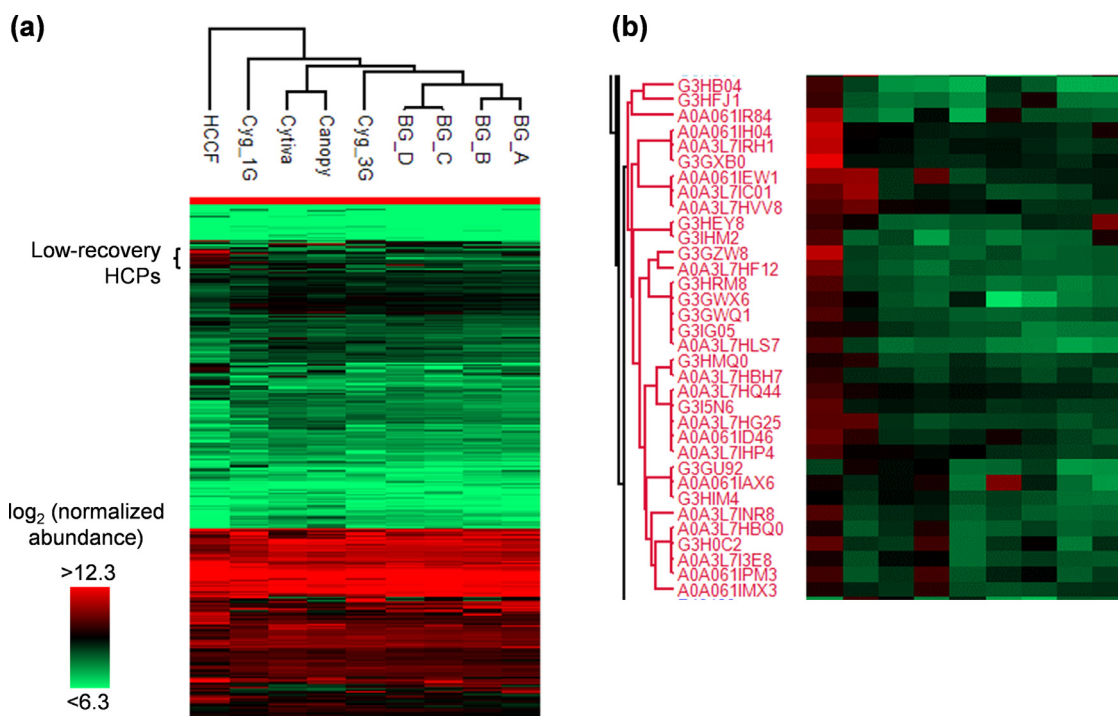


**Fig. 2.** Enrichment profiles upon affinity purification with 8 different antibodies. Hierarchical cluster analysis using  $\log_2(\text{normalized abundance})$  was conducted for proteins immunoprecipitated by 8 different antibodies and their starting materials, i.e., HCCF. Rows and columns indicate proteins and samples, respectively. (a) Overall image. Abbreviations of samples are as follows, BG\_A: BioGenes Type A, BG\_B: BioGenes Type B, BG\_C: BioGenes Type C, BG\_D: BioGenes Type D, Cyg\_1G: Cygnus 1G, Cyg\_3G: Cygnus 3G. (b) Enlarged image of "low-recovery HCPs" shown in (a). The red cluster corresponds to low-recovery HCPs.

### 3.4. Characterization of low-recovery HCPs

We examined a wide range of properties to characterize the low-recovery HCPs, including molecular weight, isoelectric point, hydrophobicity (GRAVY) [52], *in vivo* protein instability (instability index) [53], and amino acid sequence similarity to the homolog of the host animal (CovSim score). The results are shown in Fig. 3 and Suppl. Table 5. Statistically significant differences were observed for molecular weight, isoelectric point, and hydrophobicity (GRAVY) between the low-recovery HCPs and the other HCPs. On the other hand, no significant difference was observed for the instability index or CovSim score. Note that these six indices are independent of each other, except for the CovSim scores for the two host animals (goat and rabbit).

The molecular weight of low-recovery HCPs was shifted toward the lower-molecular-weight side (Fig. 3a). It is well known empirically that it is difficult to raise anti-HCP antibodies against low-molecular-weight proteins [26,28]. In the production of BioGenes Types B and D, the low-molecular-weight fraction was added to the HCCF as the antigen, but the results were not different from their counterparts (BioGenes Type A and C) prepared without spiking the low-molecular-weight fraction (Fig. 2b). The reason for the low immunogenicity of low-molecular-weight proteins may be that they have fewer potential epitopes than high-molecular-weight proteins.

It is known empirically that proteins with extreme isoelectric points have poor "coverage", and Waldera-Lupa et al. noted that acidic or basic proteins may be more easily denatured than others, making it difficult to produce antibodies that properly recognize the protein [28]. On the other hand, Henry et al. pointed out that the basic proteins identified in their study ( $pI > 9.0$ ) are often low-molecular-weight proteins, and they suggested that this might be an artifact of the analysis [26]. In the present study, acidic pro-

teins were enriched in the low-recovery HCPs (Fig. 3b), but no correlation between isoelectric point and molecular weight was observed.

As shown in Fig. 3c, hydrophilic proteins were enriched in the low-recovery HCPs. Stimulation of B cells by CD4+ T cells is a key process in the production of anti-HCP antibodies in the host animal body. CD4+ T cells recognize antigens presented by major histocompatibility complex (MHC) class II, and thus the stability of the MHC class II-peptide complex is a factor affecting anti-HCP antibody production. Since the binding of MHC class II to antigenic peptides involve hydrophobic interactions [54], it is likely that low-recovery HCPs are enriched for less hydrophobic proteins.

Although there was no statistically significant difference in *in vivo* protein instability (instability index), a shift in distribution was observed between the low-recovery HCPs and other proteins, with the third quartile of the low-recovery HCPs being above the threshold at which a protein is considered to be unstable intracellularly (Fig. 3d) [53]. It has been suggested that if a protein is extremely unstable, it may be degraded in early endosomes before reaching the antigen-processing compartment where the MHC molecules reside, resulting in low immunogenicity [55].

In general, proteins from other organisms are recognized by an organism as non-self, thus triggering an immune response. The degree of similarity between CHO cell-derived proteins and their host animal homologs may be a factor influencing affinity for the antigen. Since the low-recovery HCPs are presumed to be a subset of HCPs with low immunogenicity, the low-recovery HCPs were expected to have high similarity with their host animal homologs. However, no difference was observed in terms of CovSim scores (Fig. 3e, f). Therefore, protein similarity to the host animal homolog is not a valid indicator for predicting the reactivity of anti-HCP antibodies to HCPs.

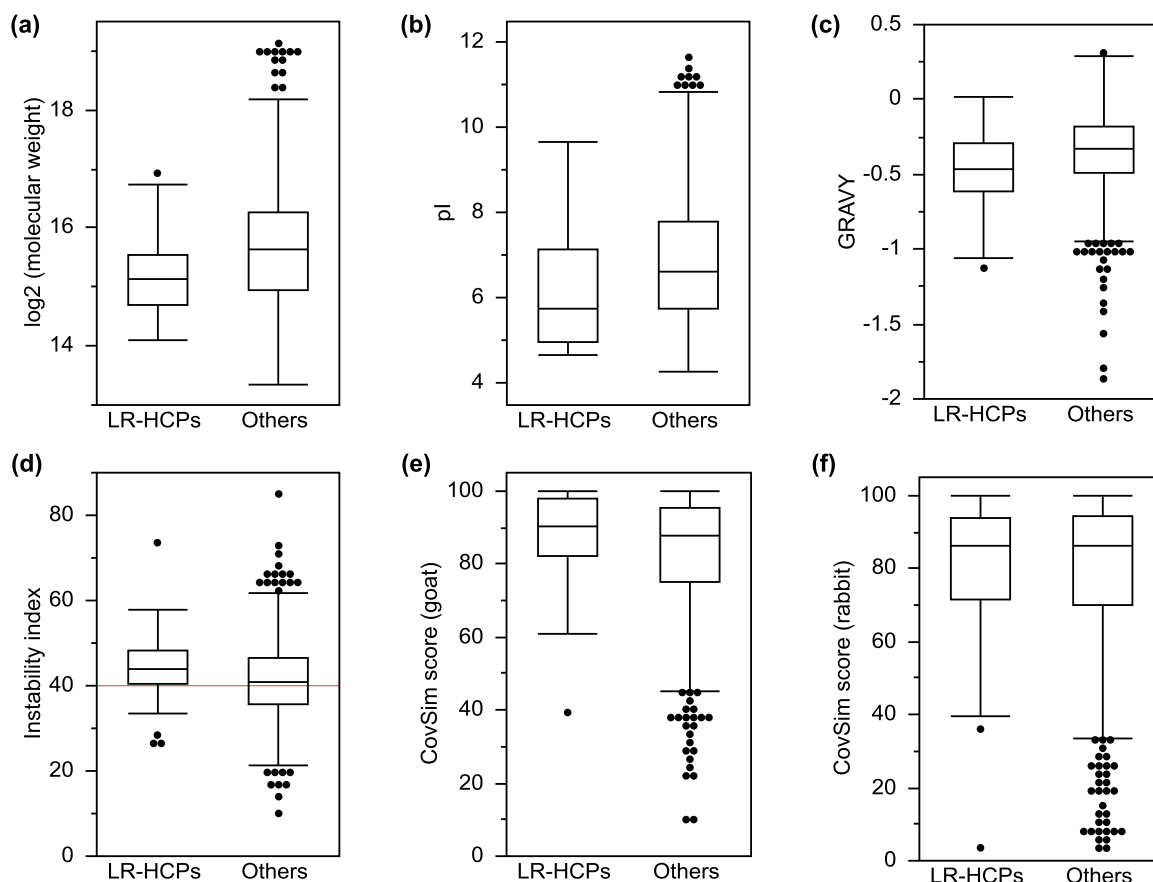


**Fig. 3.** Comparison of physico-chemical and other properties of 34 low-recovery HCPs (LR-HCPs) and 850 other HCPs. Profiles of (a)  $\log_2$  (molecular weight), (b)  $pI$ , (c) GRAVY, (d) instability index (the red line indicates the threshold at which a protein is considered unstable *in vivo*, score > 40), (e) CovSim score for goat, and (f) CovSim score for rabbit.

#### 4. Conclusions

In this study, a novel AP-MS workflow, iLAP-MS with stable isobaric labeling, was developed. This iLAP-MS method is more accurate than the previously utilized label-free quantification, and provides higher sensitivity for statistical determination. Using iLAP-MS, we simultaneously evaluated the immunoreactivity profiles of eight commercial anti-HCP antibodies with different host animals and the antigens used for immunization. As a result, we identified a group of proteins that are abundant in the HCCF but have low affinity to the antibodies, resulting in low recoveries. This group was significantly enriched in proteins exhibiting low molecular weight, low isoelectric point, and low hydrophobicity. Our results indicate that iLAP-MS is an excellent method for analyzing the immunoreactivity profiles of anti-HCP antibodies with high sensitivity and reliability. These results are expected to be useful to improve HCP control strategies in biopharmaceutical development, thereby contributing to the delivery of safe drugs to patients.

#### Data Availability

Data will be made available on request.

#### Declaration of Competing Interest

Shunsuke Takagi, Masayoshi Shibata, and Nobuyuki Suzuki are employees of Daiichi Sankyo Co., Ltd.

#### CRediT authorship contribution statement

**Shunsuke Takagi:** Conceptualization, Investigation, Writing – original draft, Visualization. **Masayoshi Shibata:** Methodology, Resources, Writing – original draft. **Nobuyuki Suzuki:** Writing – review & editing, Supervision. **Yasushi Ishihama:** Conceptualization, Writing – review & editing, Supervision, Funding acquisition, Project administration.

#### Data Availability

Data will be made available on request.

#### Acknowledgements

We wish to thank Hiroyuki Sakashita (Daiichi Sankyo Co., Ltd.) for providing the HCCF used in this study. This work was supported by the JST Strategic Basic Research Program, CREST (grant No. 18070870) to Y.I. and by a JSPS Grants-in-Aid for Scientific Research (No. 21H02459) to Y.I.

#### Supplementary materials

Supplementary material associated with this article can be found, in the online version, at doi:[10.1016/j.chroma.2022.463645](https://doi.org/10.1016/j.chroma.2022.463645).

## References

- [1] Residual host cell protein measurement in biopharmaceuticals, in: United States Pharmacopeia and National Formulary (USP-NF 2022), Issue 1, The United States Pharmacopeial Convention., Rockville, MD, 2022.
- [2] Host-cell protein assays EUROPEAN PHARMACOPEIA 10.8, European Pharmacopoeia Commission, 2022.
- [3] Host cell protein assay Japanese Pharmacopoeia 18th Edition General Information, The Ministry of Health, Labour and Welfare, Tokyo, Japan, 2021.
- [4] M. Vanderlaan, J. Zhu-Shimoni, S. Lin, F. Gunawan, T. Waerner, K.E. Van Cott, Experience with host cell protein impurities in biopharmaceuticals, *Biotechnol. Prog.* 34 (2018) 828–837.
- [5] K.M. Champion, H. Madden, J. Dougherty, E. Shacter, Defining your product profile and maintaining control over it, part 2: challenges of monitoring host cell protein impurities, *BioProcess International* (2005) 52–56.
- [6] S.K. Fischer, M. Cheu, K. Peng, J. Lowe, J. Araujo, E. Murray, D. McClintock, B. Matthews, P. Siguenza, A. Song, Specific immune response to phospholipase B-Like 2 protein, a host cell impurity in Lebrikizumab clinical material, *AAPS J.* 19 (2017) 254–263.
- [7] F. Robert, H. Bierau, M. Rossi, D. Agugiaro, T. Soranzo, H. Broly, C. Mitchell-Loegan, Degradation of an Fc-fusion recombinant protein by host cell proteases: identification of a CHO cathepsin D protease, *Biotechnol. Bioeng.* 104 (2009) 1132–1141.
- [8] S.X. Gao, Y. Zhang, K. Stansberry-Perkins, A. Buko, S. Bai, V. Nguyen, M.L. Brader, Fragmentation of a highly purified monoclonal antibody attributed to residual CHO cell protease activity, *Biotechnol. Bioeng.* 108 (2011) 977–982.
- [9] J.S. Bee, L.M. Machiesky, L. Peng, K.C. Jusino, M. Dickson, J. Gill, D. Johnson, H.-Y. Lin, K. Miller, J. Heidbrink Thompson, R.L. Remmele Jr, Identification of an IgG CDR sequence contributing to co-purification of the host cell protease cathepsin D, *Biotechnol. Prog.* 33 (2017) 140–145.
- [10] N. Dixit, N. Salamat-Miller, P.A. Salinas, K.D. Taylor, S.K. Basu, Residual host cell protein promotes polysorbate 20 Degradation in a sulfatase drug product leading to free fatty acid particles, *J. Pharm. Sci.* 105 (2016) 1657–1666.
- [11] J. Chiu, K.N. Valente, N.E. Levy, L. Min, A.M. Lenhoff, K.H. Lee, Knockout of a difficult-to-remove CHO host cell protein, lipoprotein lipase, for improved polysorbate stability in monoclonal antibody formulations, *Biotechnol. Bioeng.* 114 (2017) 1006–1015.
- [12] K.M. Champion, J.C. Nishihara, J.C. Joly, D. Arnott, Similarity of the *Escherichia coli* proteome upon completion of different biopharmaceutical fermentation processes, *Proteomics* 1 (2001) 1133–1148.
- [13] D.C. Krawitz, W. Forrester, G.T. Moreno, J. Kittleson, K.M. Champion, Proteomic studies support the use of multi-product immunoassays to monitor host cell protein impurities, *Proteomics* 6 (2006) 94–110.
- [14] J. Zhu-Shimoni, C. Yu, J. Nishihara, R.M. Wong, F. Gunawan, M. Lin, D. Krawitz, P. Liu, W. Sandoval, M. Vanderlaan, Host cell protein testing by ELISAs and the use of orthogonal methods, *Biotechnol. Bioeng.* 111 (2014) 2367–2379.
- [15] G. Rey, M.W. Wendeler, Full automation and validation of a flexible ELISA platform for host cell protein and protein A impurity detection in biopharmaceuticals, *J. Pharm. Biomed. Anal.* 70 (2012) 580–586.
- [16] C.E. Doneanu, A. Xenopoulos, K. Fadgen, J. Murphy, S.J. Skilton, H. Prentice, M. Stapels, W. Chen, Analysis of host-cell proteins in biotherapeutic proteins by comprehensive online two-dimensional liquid chromatography/mass spectrometry, *MAbs* 4 (2012) 24–44.
- [17] M.R. Schenauer, G.C. Flynn, A.M. Goetze, Identification and quantification of host cell protein impurities in biotherapeutics using mass spectrometry, *Anal. Biochem.* 428 (2012) 150–157.
- [18] L. Huang, N. Wang, C.E. Mitchell, T. Brownlee, S.R. Maple, M.R. De Felippis, A novel sample preparation for shotgun proteomics characterization of HCPs in antibodies, *Anal. Chem.* 89 (2017) 5436–5444.
- [19] X. Gao, B. Rawal, Y. Wang, X. Li, D. Wylie, Y.-H. Liu, L. Breunig, D. Driscoll, F. Wang, D.D. Richardson, Targeted host cell protein quantification by LC-MRM enables biologics processing and product characterization, *Anal. Chem.* 92 (2020) 1007–1015.
- [20] S. Nie, T. Greer, R. O'Brien Johnson, X. Zheng, A. Torri, N. Li, Simple and sensitive method for deep profiling of host cell proteins in therapeutic antibodies by combining Ultra-Low Trypsin concentration digestion, long chromatographic gradients, and BoxCar mass spectrometry acquisition, *Anal. Chem.* 93 (2021) 4383–4390.
- [21] Z. Shahrokh, D. Schmalzing, R. Rawat, V. Sluzky, K. Ho, J. Engelbergs, J. Bishop, E. Friedl, B. Meiklejohn, N. Ritter, Science, risks, and regulations: current perspectives on host cell protein analysis and control, *Bioprocess Int.* 14 (2016) 40–51.
- [22] X. Wang, A.K. Hunter, N.M. Mozier, Host cell proteins in biologics development: identification, quantitation and risk assessment, *Biotechnol. Bioeng.* 103 (2009) 446–458.
- [23] F. Chevalier, Highlights on the capacities of “Gel-based” proteomics, *Proteome Sci* 8 (2010) 23.
- [24] A.L. Tscheliessnig, J. Konrath, R. Bates, A. Jungbauer, Host cell protein analysis in therapeutic protein bioprocessing - methods and applications, *Biotechnol. J.* 8 (2013) 655–670.
- [25] M. Kornecki, F. Mestmäcker, S. Zobel-Roos, L. Heikaus de Figueiredo, H. Schlüter, J. Strube, Host cell proteins in biologics manufacturing: the good, the bad, and the Ugly, *Antibodies (Basel)* 6 (2017), doi:10.3390/antib6030013.
- [26] S.M. Henry, E. Sutlief, O. Salas-Solano, J. Valliere-Douglass, ELISA reagent coverage evaluation by affinity purification tandem mass spectrometry, *MAbs* 9 (2017) 1065–1075.
- [27] K. Pilely, S.B. Nielsen, A. Draborg, M.L. Henriksen, S.W.K. Hansen, L. Skriver, E. Mørtz, R.R. Lund, A novel approach to evaluate ELISA antibody coverage of host cell proteins—combining ELISA-based immunocapture and mass spectrometry, *Biotechnol. Prog.* 36 (2020) e2983.
- [28] D.M. Waldera-Lupa, Y. Jasper, P. Köhne, R. Schwichtenhövel, H. Falkenberg, T. Flad, P. Happersberger, B. Reisinger, A. Dehghani, R. Moussa, T. Waerner, Host cell protein detection gap risk mitigation: quantitative IAC-MS for ELISA antibody reagent coverage determination, *MAbs* 13 (2021) 1955432.
- [29] C. Seisenberger, T. Graf, M. Haindl, H. Wegele, M. Wiedmann, S. Wohlrab, Questioning coverage values determined by 2D western blots: a critical study on the characterization of anti-HCP ELISA reagents, *Biotechnol. Bioeng.* 118 (2021) 1116–1126.
- [30] C. Seisenberger, T. Graf, M. Haindl, H. Wegele, M. Wiedmann, S. Wohlrab, Toward optimal clearance - a universal affinity based mass spectrometry approach for comprehensive ELISA reagent coverage evaluation and HCP hitchhiker analysis, *Biotechnol. Prog.* (2022) e3244.
- [31] S.-E. Ong, B. Blagoev, I. Kratchmarova, D.B. Kristensen, H. Steen, A. Pandey, M. Mann, Stable isotope labeling by amino acids in cell culture, SILAC, as a simple and accurate approach to expression proteomics, *Mol. Cell. Proteomics* 1 (2002) 376–386.
- [32] A. Thompson, J. Schäfer, K. Kuhn, S. Kienle, J. Schwarz, G. Schmidt, T. Neumann, R. Johnstone, A.K.A. Mohammed, C. Hamon, Tandem mass tags: a novel quantitative strategy for comparative analysis of complex protein mixtures by MS/MS, *Anal. Chem.* 75 (2003) 1895–1904.
- [33] J.-L. Hsu, S.-Y. Huang, N.-H. Chow, S.-H. Chen, Stable-isotope dimethyl labeling for quantitative proteomics, *Anal. Chem.* 75 (2003) 6843–6852.
- [34] S. Wiese, K.A. Reidegeld, H.E. Meyer, B. Warscheid, Protein labeling by iTRAQ: a new tool for quantitative mass spectrometry in proteome research, *Proteomics* 7 (2007) 340–350.
- [35] Z. Li, R.M. Adams, K. Chourey, G.B. Hurst, R.L. Hettich, C. Pan, Systematic comparison of label-free, metabolic labeling, and isobaric chemical labeling for quantitative proteomics on LTQ Orbitrap Velos, *J. Proteome Res.* 11 (2012) 1582–1590.
- [36] H. Wang, S. Alvarez, L.M. Hicks, Comprehensive comparison of iTRAQ and label-free LC-based quantitative proteomics approaches using two *Chlamydomonas reinhardtii* strains of interest for biofuels engineering, *J. Proteome Res.* 11 (2012) 487–501.
- [37] A. Hogrebe, L. von Stechow, D.B. Bekker-Jensen, B.T. Weinert, C.D. Kelstrup, J.V. Olsen, Benchmarking common quantification strategies for large-scale phosphoproteomics, *Nat. Commun.* 9 (2018) 1045.
- [38] A. Thompson, N. Wölmer, S. Koncarevic, S. Selzer, G. Böhm, H. Legner, P. Schmid, S. Kienle, P. Penning, C. Höhle, A. Berfelde, R. Martinez-Pinna, V. Farztdinov, S. Jung, K. Kuhn, I. Pike, TMTpro: design, synthesis, and initial evaluation of a proline-based isobaric 16-Plex tandem mass tag reagent set, *Anal. Chem.* 91 (2019) 15941–15950.
- [39] T. Okumura, K. Masuda, K. Watanabe, K. Miyadai, K. Nonaka, M. Yabuta, T. Omasa, Efficient enrichment of high-producing recombinant Chinese hamster ovary cells for monoclonal antibody by flow cytometry, *J. Biosci. Bioeng.* 120 (2015) 340–346.
- [40] T. Masuda, M. Tomita, Y. Ishihama, Phase transfer surfactant-aided trypsin digestion for membrane proteome analysis, *J. Proteome Res.* 7 (2008) 731–740.
- [41] J. Rappsilber, Y. Ishihama, M. Mann, Stop and go extraction tips for matrix-assisted laser desorption/ionization, nanoelectrospray, and LC/MS sample pretreatment in proteomics, *Anal. Chem.* 75 (2003) 663–670.
- [42] S. Tyanova, T. Temu, P. Sinitcyn, A. Carlson, M.Y. Hein, T. Geiger, M. Mann, J. Cox, The Perseus computational platform for comprehensive analysis of (pro)teomics data, *Nat. Methods.* 13 (2016) 731–740.
- [43] Y.H. Benjamini, Y. Hochberg, Controlling the false discovery rate - a practical and powerful approach to multiple testing, *J. R. Stat. Soc. Ser. B: Methodol.* 57 (1995) 289–300.
- [44] D.L. Plubell, P.A. Wilmarth, Y. Zhao, A.M. Fenton, J. Minnier, A.P. Reddy, J. Klimek, X. Yang, L.L. David, N. Pamir, Extended multiplexing of Tandem Mass Tags (TMT) labeling reveals age and high fat diet specific proteome changes in mouse epididymal adipose tissue, *Mol. Cell. Proteomics* 16 (2017) 873–890.
- [45] B. Chapman, J. Chang, Biopython: Python tools for computational biology, *SIG-BIO News* 20 (2000) 15–19.
- [46] P.J.A. Cock, T. Antao, J.T. Chang, B.A. Chapman, C.J. Cox, A. Dalke, I. Friedberg, T. Hamelryck, F. Kauff, B. Wilczynski, M.J.L. de Hoon, Biopython: freely available Python tools for computational molecular biology and bioinformatics, *Bioinformatics* 25 (2009) 1422–1423.
- [47] S.F. Altschul, T.L. Madden, A.A. Schäffer, J. Zhang, Z. Zhang, W. Miller, D.J. Lipman, Gapped BLAST and PSI-BLAST: a new generation of protein database search programs, *Nucl. Acids Res* 25 (1997) 3389–3402.
- [48] C. Camacho, G. Coulouris, V. Avagyan, N. Ma, J. Papadopoulos, K. Bealer, T.L. Madden, BLAST+: architecture and applications, *BMC Bioinform.* 10 (2009) 421.
- [49] S. Holm, A simple sequentially rejective multiple test procedure, *Scand. Stat. Theory Appl.* 6 (1979) 65–70.
- [50] K. Bomans, A. Lang, V. Roedel, L. Adolf, K. Kyrioglou, K. Diepold, G. Eberl, M. Mølhøj, U. Strauss, C. Schmalz, R. Vogel, D. Reusch, H. Wegele, M. Wiedmann, P. Bulau, Identification and monitoring of host cell proteins by mass spectrometry combined with high performance immunochemistry testing, *PLoS One* 8 (2013) e81639.
- [51] Q. Zhang, A.M. Goetze, H. Cui, J. Wylie, S. Trimble, A. Hewig, G.C. Flynn, Comprehensive tracking of host cell proteins during monoclonal antibody purifications using mass spectrometry, *MAbs* 6 (2014) 659–670.



- [52] J. Kyte, R.F. Doolittle, A simple method for displaying the hydropathic character of a protein, *J. Mol. Biol.* 157 (1982) 105–132.
- [53] K. Guruprasad, B.V. Reddy, M.W. Pandit, Correlation between stability of a protein and its dipeptide composition: a novel approach for predicting in vivo stability of a protein from its primary sequence, *Protein Eng* 4 (1990) 155–161.
- [54] A. Ferrante, J. Gorski, Cooperativity of hydrophobic anchor interactions: evidence for epitope selection by MHC class II as a folding process, *J. Immunol.* 178 (2007) 7181–7189.
- [55] S. Scheiblhofer, J. Laimer, Y. Machado, R. Weiss, J. Thalhamer, Influence of protein fold stability on immunogenicity and its implications for vaccine design, *Expert Rev. Vaccines.* 16 (2017) 479–489.